A Block-by-Block Blind Post-FFT Multistage Beamforming Algorithm for Multiuser OFDM Systems Based on Subcarrier Averaging

Chong-Yung Chi, Chun-Hsien Peng, Kuan-Chang Huang, Teng-Han Tsai, and Wing-Kin Ma

***Abstract*—Chi *et al.* proposed a computationally efficient fast kurtosis maximization algorithm for blind equalization of multiple-input multiple-output linear time-invariant systems. This algorithm is also an iterative batch processing algorithm and has been applied to blind source separation. This paper considers blind beamforming of multiuser orthogonal frequency division multiplexing (OFDM) systems. Assuming that the channel is static within one OFDM block, a blind post-FFT multistage beamforming algorithm (MSBFA) based on subcarrier averaging is proposed. The algorithm basically comprises: i) source (path signal) extraction using a hybrid beamforming algorithm composed of a Fourier beamformer and a kurtosis maximization beamformer, ii) time delay estimation and compensation, iii) classification (path-to-user association) and blind maximum ratio combining (of path signals). The designed beamformer is exactly the same for all the subcarriers, effectively utilizes multipath diversity for performance gain, and works well even in an environment with spatially correlated sources. Some simulation results are presented to demonstrate the effectiveness of the proposed MSBFA.**

***Index Terms*—Orthogonal frequency division multiplexing (OFDM), pre-FFT beamforming structure, post-FFT beamforming structure, Fourier beamformer, kurtosis maximization, blind maximum ratio combining (BMRC).**

I. INTRODUCTION

THE need for high transmission rate and guaranteed quality of service has grown rapidly in wireless communication systems. To meet this need, orthogonal frequency division multiplexing (OFDM) has been considered one of the major techniques for next generation mobile communications [1], [2]. It has been widely known that a receiver of OFDM systems can avoid intersymbol interference if the guard interval (GI) is larger than the channel delay profile. The OFDM has been adopted in digital audio broadcasting (DAB) and digital video broadcasting-terrestrial (DVB-T), as well as wireless local area networks (WLANs) such as IEEE 802.11a and HIPERLAN [1], [3]–[8].

To maintain high-speed reliable radio transmission with a limited bandwidth, the use of antenna arrays (or multiple antennas) has been considered not only for antenna gain (or spatial diversity gain) as well as increase of spectral efficiency, but also for interference suppression [1], [6], [8], [9]. Therefore, OFDM in conjunction with multiple-input multiple-output (MIMO) signal processing has naturally been proposed for broadband communications, especially in the beamforming design of the receiver, such as the pre-FFT beamforming structure (pre-FFT BFS) (as shown in Figure 1(a)) [1], [5]–[7], and post-FFT beamforming structure (post-FFT BFS) (as shown in Figure 1(b)) [4]–[8].

A number of nonblind and blind beamforming algorithms for multiuser OFDM systems equipped with an antenna array have been reported in the open literature. Nonblind algorithms such as maximum ratio combining (MRC) [4], [6] and minimum mean square error (MMSE) beamformers [1], [5], [6], [9] require the channel to be estimated in advance through the use of training sequences or pilot signals, consequently resulting in reduced spectral efficiency. Therefore, blind algorithms with no need of pilot signals may be preferable.

Capon's minimum variance (MV) beamformer [9]–[12] has been popularly used for blind beamforming in the areas of array signal processing and wireless communications. Although the MV beamformer can suppress strong interfering signals, it needs the direction of arrival (DOA) of the signal of interest beforehand. Moreover, the MV beamformer fails to work if there exist spatially correlated source signals (from different DOAs with the same arrival time at the receiving antenna array) [9], [11]–[15]. Some multiple linear constrained methods [12]–[14], [16] and spatial smoothing methods [11], [15] have been proposed to resolve the issue of spatially correlated source signals, provided that DOAs of spatially correlated source signals are known or can be estimated in advance. Nevertheless, even if the above issue can be effectively solved, the performance of the MV beamformer is limited due to the lack of multipath diversity. A prominent merit of the MV beamformer as applied to the pre-FFT BFS is that it is a block-by-block processing algorithm (i.e., only one OFDM block is needed rather than a set of OFDM blocks), in contrast to blind beamforming algorithms based on the post-

Manuscript received March 7, 2007; revised July 11, 2007 and October 7, 2007; accepted November 21, 2007. The associate editor coordinating the review of this paper and approving it for publication was X. Gao. This work was supported by the National Science Council, R.O.C., under Grants NSC 95-2219-E-007-004 and 96-2219-E-007-004. This work was partly presented at the 2005 International Symposium on Intelligent Signal Processing and Communication Systems (ISPACS), Hong Kong, Dec. 13-16, 2005, and partly presented at the 8th IEEE Workshop on Signal Processing Advances in Wireless Communications (SPAWC), Helsinki, Finland, June 17-20, 2007.

C.-Y. Chi (the corresponding author) is with the Institute of Communications Engineering and the Department of Electrical Engineering, National Tsing Hua University, Hsinchu, Taiwan, R.O.C. (e-mail: cychi@ee.nthu.edu.tw).

C.-H. Peng, K.-C. Huang, and T.-H. Tsai are with the Institute of Communications Engineering, National Tsing Hua University, Hsinchu, Taiwan, R.O.C.

W.-K. Ma is with the Department of Electronic Engineering, The Chinese University of Hong Kong, Shatin, N.T., Hong Kong (e-mail: wkma@ieee.org).

Digital Object Identifier 10.1109/TWC.2008.070269.

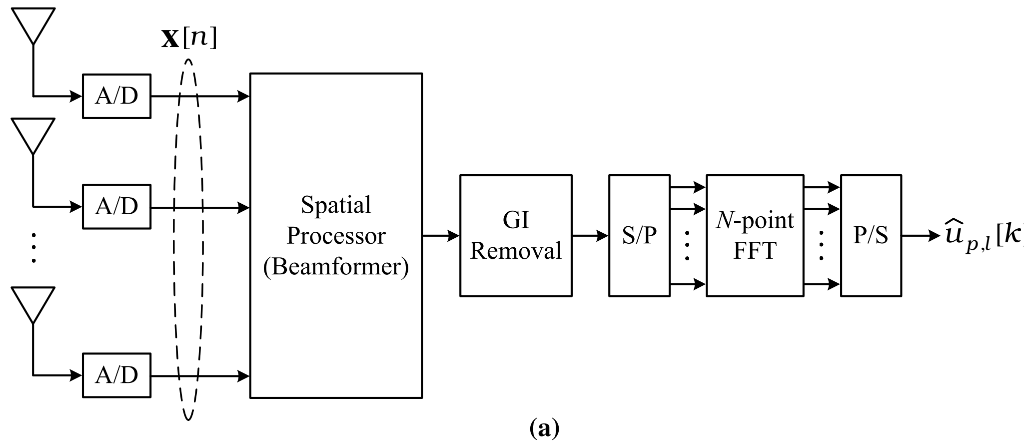

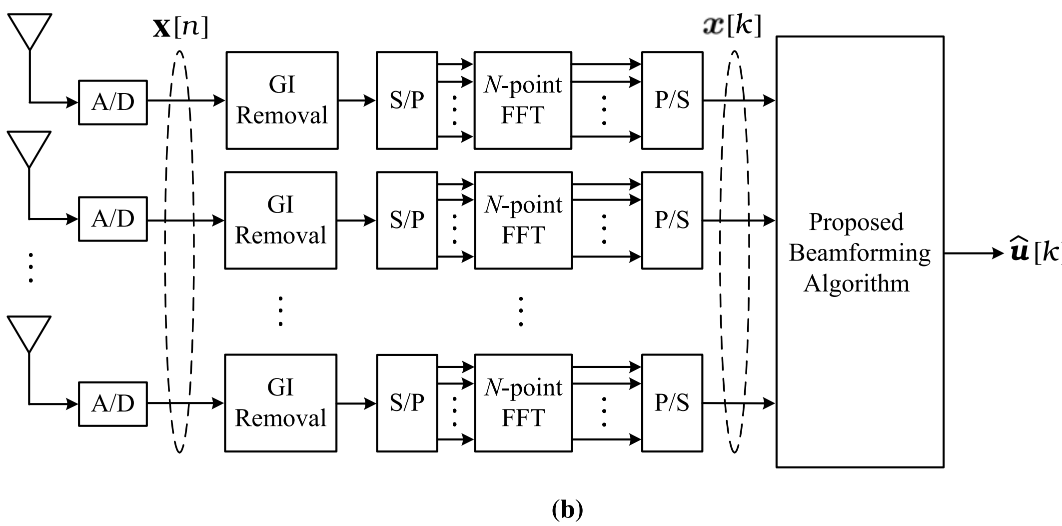

Fig. 1. Block diagrams for (a) Pre-FFT BFS and (b) Post-FFT BFS.

FFT BFS as reported in [2], [8], [17].

Blind beamforming algorithms associated with the post-FFT BFS have also been reported in the open literature such as the blind adaptive constant modulus algorithm [8] and subspace-based methods [2], [17] for which blind channel estimation is performed prior to the design of beamformer for each subcarrier using multiple OFDM blocks. In other words, a set of N beamformers (where N is the total number of subcarriers) each for a subcarrier is needed in addition to multiple OFDM blocks (which further require the channel to be static over these OFDM blocks). Therefore, it is desirable to design a block-by-block blind beamforming algorithm which is exactly the same for all the subcarriers and attains maximum multipath diversity gain at the same time.

Recently, Chi *et al.* [18]–[22] proposed a computationally efficient fast kurtosis (a fourth-order statistic) maximization algorithm (FKMA) with super-exponential convergence rate and guaranteed convergence. It has been successfully applied to blind beamforming, blind source separation (or independent component analysis), and blind maximum ratio combining (BMRC). The FKMA is not applicable to the MIMO model associated with the pre-FFT BFS (since the model inputs are approximately Gaussian). However, the FKMA is applicable to the post-FFT BFS but it requires a set of N beamformers each for a subcarrier and the channel to be static over multiple OFDM blocks. In this paper, we propose a block-by-block blind *Multistage Beamforming Algorithm* (MSBFA) associated with the post-FFT BFS based on subcarrier averaging over one OFDM block. The designed beamformer is exactly the same for all the subcarriers, effectively utilizes multipath diversity for performance gain, and is applicable in the presence of spatially correlated sources.

The remaining parts of the paper are organized as follows. Section 2 reviews discrete-time instantaneous MIMO models associated with the pre-FFT BFS and post-FFT BFS. Section 3 presents a hybrid source extraction scheme which is needed in the proposed blind MSBFA to be presented in Section 4. In Section 5, we show some simulation results to support the effectiveness of the proposed blind MSBFA. Finally, some conclusions are drawn in Section 6.

II. MIMO Models for Beamforming of Multiuser OFDM Systems

For ease of later use, let us define the following notations:

n	Discrete-time (sample) index
k	Frequency bin (subcarrier) index
$E\{\cdot\}$	Expectation operator

$\|\cdot\|$	Euclidean norm of vectors or matrices
$\mathbf{I}_M$	$M \times M$ identity matrix
c^*	Complex conjugate of a complex number c
$\theta_{p,l}$	$(-\pi/2 \le \theta_{p,l} \le \pi/2)$ DOA associated with the lth path of user p
$\mathbf{a}(\theta_{p,l})$	$Q \times 1$ steering vector associated with DOA $\theta_{p,l}$
$\alpha_{p,l}$	Path gain associated with DOA $\theta_{p,l}$
$\tau_{p,l}$	Time delay associated with DOA $\theta_{p,l}$ in discrete-time domain after sampling
L_p	Total number of paths (or DOAs) associated with user p
L	$(= L_1 + L_2 + \cdots + L_P)$ total number of paths (or DOAs) of all the users.

Consider the uplink of a quasi-synchronous multiuser OFDM system [2], [17], [23] (for which all the paths of all the users fall within the GI) with P active users operating in outdoor rural environments. At the transmitter (equipped with a single antenna) of the user p, the data sequence $u_p[k]$ is processed by serial-to-parallel (S/P) conversion, N-point IFFT operation, parallel-to-serial (P/S) conversion, and insertion of a GI of length equal to N_g. Then the transmitted OFDM signal of user p can be expressed as [3]

$$s_p[n] = \frac{1}{N}\sum_{k=0}^{N-1} u_p[k] e^{j2\pi kn/N} \tag{1}$$

for $n = -N_g$, $-N_g + 1$, ..., $N-1$, where $u_p[k]$ is the data sequence of user p.

Assume that the channel is invariant within one OFDM block and so are DOA $\theta_{p,l}$, path gain $\alpha_{p,l}$ and time delay $\tau_{p,l}$. The receiver at the base station is equipped with a uniform linear antenna array of Q elements equally spaced by half a carrier wavelength. The received baseband discrete-time signal can be expressed as

$$\mathbf{x}[n] = \sum_{p=1}^{P}\sum_{l=1}^{L_p} \alpha_{p,l}\mathbf{a}(\theta_{p,l}) s_p[n-\tau_{p,l}] + \mathbf{w}[n] \tag{2}$$

for $n = -N_g, ..., N-1$, where $\mathbf{w}[n]$ is a $Q \times 1$ noise vector and

$$\mathbf{a}(\theta_{p,l}) = (1, e^{-j\pi \sin(\theta_{p,l})}, ..., e^{-j(Q-1)\pi \sin(\theta_{p,l})})^{\mathrm{T}}. \tag{3}$$

Next, let us make some general assumptions for the received signal $\mathbf{x}[n]$ given by (2) as follows:

(A1) $u_1[k]$, $u_2[k]$, ..., $u_P[k]$ are mutually independent identically distributed (i.i.d.) quadriphase-shift keying (QPSK) symbol sequences (i.e., $u_p[k]$ for each k is a random variable with uniform probability mass function over the sample description space $\{\pm e^{j\pi/4}, \pm e^{-j\pi/4}\}$).

(A2) $\theta_{q,m} \neq \theta_{p,l}$ for all $(q,m) \neq (p,l)$ and $Q \ge L$.

(A3) $\tau_{p,l} \in \{0, ..., N_g\}$ for all p and l (quasi-synchronous OFDM system) and $\tau_{p,1} < \cdots < \tau_{p,L_p}$.

(A4) $\mathbf{w}[n]$ is zero-mean Gaussian with $E\{\mathbf{w}[n]\mathbf{w}^{\mathrm{H}}[n]\} = \sigma_w^2 \mathbf{I}_Q$, and is statistically independent of $u_p[k]$, $p = 1, 2, ..., P$.

Next, let us present the MIMO models associated with the two widely known beamforming structures of OFDM systems mentioned in the introduction section: the pre-FFT BFS as shown in Figure 1(a) and the post-FFT BFS as shown in Figure 1(b).

A. MIMO Model for Pre-FFT BFS

For the pre-FFT BFS [1], [5]–[7] (see Figure 1(a)), the baseband discrete-time received signal $\mathbf{x}[n]$ given by (2) can be expressed as a $Q \times L$ instantaneous MIMO model

$$\mathbf{x}[n] = \mathbf{A}\mathbf{s}[n] + \mathbf{w}[n], \quad n = -N_g, -N_g+1, ..., N-1, \tag{4}$$

where

$$\begin{aligned}\mathbf{A} &= (\mathbf{A}_1, \mathbf{A}_2, ..., \mathbf{A}_P) \\ &= (\boldsymbol{a}^{(1)}, \boldsymbol{a}^{(2)}, ..., \boldsymbol{a}^{(L)}), \quad Q \times L \text{ matrix}\end{aligned} \tag{5}$$

$$\begin{aligned}\mathbf{s}[n] &= (\mathbf{s}_1^{\mathrm{T}}[n], \mathbf{s}_2^{\mathrm{T}}[n], ..., \mathbf{s}_P^{\mathrm{T}}[n])^{\mathrm{T}} \\ &= (s^{(1)}[n], s^{(2)}[n], ..., s^{(L)}[n])^{\mathrm{T}}, \quad L \times 1 \text{ vector}\end{aligned} \tag{6}$$

are the $Q \times L$ mixing matrix (or DOA matrix) and the $L \times 1$ input vector consisting of L source signals, respectively, in which

$$\mathbf{A}_p = (\alpha_{p,1}\mathbf{a}(\theta_{p,1}), \alpha_{p,2}\mathbf{a}(\theta_{p,2}), ..., \alpha_{p,L_p}\mathbf{a}(\theta_{p,L_p})), \quad Q \times L_p \text{ matrix} \tag{7}$$

$$\mathbf{s}_p[n] = (s_{p,1}[n], s_{p,2}[n], ..., s_{p,L_p}[n])^{\mathrm{T}}, \quad L_p \times 1 \text{ vector} \tag{8}$$

$$s_{p,l}[n] = s_p[n - \tau_{p,l}]. \tag{9}$$

A remark for the MIMO model $\mathbf{x}[n]$ given by (4) associated with the pre-FFT BFS is as follows:

(R1) One can observe, from (6), (8), and Assumptions (A1) and (A3), that $\mathbf{s}[n]$ *for each fixed* n is a zero-mean random vector with all the random components being mutually statistically independent with $E\{\mathbf{s}[n]\mathbf{s}^{\mathrm{H}}[n]\} = \frac{1}{N}\mathbf{I}_L$. Moreover, $\mathbf{s}[n]$ (comprising N-point IFFT of $u_p[k]$ by (1)) is approximately Gaussian by Central Limit Theorem. On the other hand, the $Q \times L$ DOA matrix $\mathbf{A}$ (see (5) and (7)) is of full column rank by Assumption (A2) and each column $\boldsymbol{a}^{(i)}$ of $\mathbf{A}$ only comprises the component from a single path. These observations imply that only second-order statistics (SOS) based blind beamforming algorithms can be applied, such as the Capon's MV beamformer and Fourier beanformer [9], but their performance is limited due to the lack of path diversity if there is no further processing for obtaining path diversity gain that involves non-trivial path gain estimation, time delay estimation and compensation, and coherent combination of the extracted path signals in the time domain.

B. MIMO Model for Post-FFT BFS

As shown in Figure 1(b), after the processes of the removal of GI, S/P conversion, N-point FFT operation, and P/S conversion at each receive antenna, the MIMO model for each subcarrier k of the post-FFT BFS can be established as follows [2], [8], [17]:

$$\begin{aligned}\boldsymbol{x}[k] &= \sum_{p=1}^{P}\sum_{l=1}^{L_p} \alpha_{p,l}\mathbf{a}(\theta_{p,l}) u_p[k] e^{-j2\pi k\tau_{p,l}/N} + \boldsymbol{w}[k] \quad \text{(by (2))} \\ &= \mathbf{A}^{(k)}\boldsymbol{u}^{(k)} + \boldsymbol{w}[k], \quad k = 0, 1, ..., N-1,\end{aligned} \tag{10}$$

where $\boldsymbol{w}[k]$ is also a $Q \times 1$ white Gaussian noise vector,

$$\boldsymbol{u}^{(k)} = (u_1[k], u_2[k], ..., u_P[k])^{\mathrm{T}}, \quad P \times 1 \text{ vector} \tag{11}$$

$$\mathbf{A}^{(k)} = (\boldsymbol{a}_1^{(k)}, \boldsymbol{a}_2^{(k)}, ..., \boldsymbol{a}_P^{(k)}), \quad Q \times P \text{ matrix} \tag{12}$$

and each column of $\mathbf{A}^{(k)}$ is given by

$$\boldsymbol{a}_p^{(k)} = \sum_{l=1}^{L_p} \alpha_{p,l} \mathbf{a}(\theta_{p,l}) e^{-j2\pi k \tau_{p,l}/N}. \tag{13}$$

A remark for the MIMO model $\boldsymbol{x}[k]$ given by (10) associated with the post-FFT BFS is as follows:

(R2) By (11) and Assumption (A1), one can observe that all the $u_p[k]$'s in $\boldsymbol{u}^{(k)}$ are zero-mean non-Gaussian mutually statistically independent. Moreover, $\mathbf{A}^{(k)}$ is of full column rank by Assumption (A2) and each column $\boldsymbol{a}_p^{(k)}$ of $\mathbf{A}^{(k)}$ comprises multipath components implying that some path diversity gain in the estimation of $u_p[k]$ may be expected but is channel dependent. Thus, blind beamforming algorithms either using SOS such as blind subspace methods [2] or using higher-order statistics (HOS) such as the conventional FKMA [18], [20] are applicable to the estimation of $u_p[k]$. However, in general, they require many OFDM data blocks under the assumption that the channel is static over these OFDM data blocks, and meanwhile a set of N beamformers is needed because of $\mathbf{A}^{(k)} \neq \mathbf{A}^{(j)}$ for all $k \neq j$, which may lead to higher computational complexity of the post-FFT BFS based beamformers compared with the pre-FFT BFS based beamformers [1], [7].

III. Source Extraction by Subcarrier Averaging

The advantages of the two beamforming structures mentioned in Section 2, low computational complexity for the pre-FFT BFS and path diversity gain for the post-FFT BFS, can be shared by re-expressing the MIMO model in (10) as

$$\boldsymbol{x}[k] = \mathbf{A}\boldsymbol{u}[k] + \boldsymbol{w}[k], \quad k = 0, 1, ..., N-1, \quad \text{(by (10) and (5))} \tag{14}$$

where the $Q \times L$ mixing matrix $\mathbf{A}$ given by (5) is the same for all k, and the $L \times 1$ source vector $\boldsymbol{u}[k]$ is defined as follows:

$$\boldsymbol{u}[k] = (\boldsymbol{u}_1^{\mathrm{T}}[k], \boldsymbol{u}_2^{\mathrm{T}}[k], ..., \boldsymbol{u}_P^{\mathrm{T}}[k])^{\mathrm{T}}, \quad L \times 1 \text{ vector} \tag{15}$$

$$\boldsymbol{u}_p[k] = (u_{p,1}[k], u_{p,2}[k], ..., u_{p,L_p}[k])^{\mathrm{T}}, \quad L_p \times 1 \text{ vector} \tag{16}$$

$$u_{p,l}[k] = u_p[k] e^{-j2\pi k \tau_{p,l}/N}. \tag{17}$$

Note that the MIMO model $\boldsymbol{x}[k]$ given by (14) (associated with the post-FFT BFS) is nothing but an instantaneous MIMO model with the same DOA matrix $\mathbf{A}$ (see (5) and (7)) associated with the MIMO model $\mathbf{x}[n]$ for the pre-FFT BFS (see (4)).

By treating the subcarrier k as the time index, it can be easily seen that each source component $u_{p,l}[k]$ of $\boldsymbol{u}[k]$ is a zero-mean wide-sense stationary complex exponential signal with unity magnitude and i.i.d. phase $\arg\{u_p[k]\} \in \{\pm\pi/4, \pm 3\pi/4\}$, and meanwhile $\boldsymbol{u}[k]$ involves correlated components associated with the same user because $E\{u_{p,l}[k]u_{p,m}^*[k]\} = e^{-j2\pi k(\tau_{p,l}-\tau_{p,m})/N} \neq 0$ for all $l \neq m$ (by (17) and Assumptions (A1) and (A3)), implying that none of the blind beamforming algorithms including the conventional FKMA can be applied. In order to overcome the issue of correlated components between $u_{p,l}[k]$ and $u_{p,m}^*[k]$ for all $l \neq m$, let us present the following lemma which is needed in the development of source extraction schemes to be presented below and its proof is given in Appendix A.

Lemma 1. *Let*

$$\langle u_{p,l}[k] \rangle = \frac{1}{N} \sum_{k=0}^{N-1} u_{p,l}[k] \tag{18}$$

denote the subcarrier average of $u_{p,l}[k]$. Under the assumptions (A1) and (A3), the following subcarrier averages converge in probability as $N \to \infty$:

$$\langle (u_{p,l}[k])^2 \rangle \xrightarrow{\mathrm{p}} 0, \quad \forall\ p \text{ and } l, \tag{19}$$

$$\langle u_{p,l}[k](u_{q,m}[k])^* \rangle \xrightarrow{\mathrm{p}} 0, \quad \forall\ (p,l) \neq (q,m), \tag{20}$$

where $\xrightarrow{\mathrm{p}}$ denotes "convergence in probability" as $N \to \infty$.

Next, let us define a notational mapping for the need in the proposed source extraction schemes as follows

$$\begin{aligned} &\{(\alpha^{(r)}, \theta^{(r)}, \tau^{(r)}, u^{(r)}[k]),\ r = 1, ..., L\} \\ &\triangleq \{(\alpha_{p,l}, \theta_{p,l}, \tau_{p,l}, u_{p,l}[k]),\ p = 1, ..., P,\ l = 1, ..., L_p\}, \end{aligned} \tag{21}$$

where the mapping between r and (p, l) is one-to-one. Moreover, let $\boldsymbol{v}$ (a $Q \times 1$ vector) denote a beamformer to be designed and let $e[k]$ denote the corresponding beamformer output, i.e.,

$$e[k] = \boldsymbol{v}^{\mathrm{H}} \boldsymbol{x}[k] = \mathbf{g}^{\mathrm{T}} \boldsymbol{u}[k] + w[k] = \sum_{r=1}^{L} g^{(r)} u^{(r)}[k] + w[k], \tag{22}$$

where $w[k] = \boldsymbol{v}^{\mathrm{H}} \boldsymbol{w}[k]$ and

$$\mathbf{g}^{\mathrm{T}} = \boldsymbol{v}^{\mathrm{H}} \mathbf{A} = (g^{(1)}, g^{(2)}, ..., g^{(L)}). \tag{23}$$

Suppose that in the presence of noise, $e[k]$ is an estimate of $u^{(r)}[k]$ up to an unknown scale factor. The input-output cross-correlation (IOCC) method by ensemble averaging [18]–[20], [24], [25] is a widely known channel estimator (but not an unbiased channel estimator) when a channel input is known or has been estimated. This motivates the IOCC channel estimation by subcarrier averaging, which is supported by the following lemma:

Lemma 2. *Under the assumptions (A1) through (A3) and the noise-free assumption,*

$$\langle \boldsymbol{x}[k](u^{(r)}[k])^* \rangle \xrightarrow{\mathrm{p}} \boldsymbol{a}^{(r)} = \alpha^{(r)} \mathbf{a}(\theta^{(r)}), \tag{24}$$

i.e., the subcarrier average based cross-correlation between $u^{(r)}[k]$ and $\boldsymbol{x}[k]$ converges in probability to $\boldsymbol{a}^{(r)} = \alpha^{(r)} \mathbf{a}(\theta^{(r)})$ as $N \to \infty$.

The proof of Lemma 2 is presented in Appendix B. Then the associated channel estimate can be expressed as follows:

$$\widehat{\boldsymbol{a}}^{(r)} = \langle \boldsymbol{x}[k] \widetilde{e}^*[k] \rangle, \quad \text{(by Lemma 2)} \tag{25}$$

where $\widetilde{e}[k]$ is the normalized beamformer output,

$$\widetilde{e}[k] = e[k]/\langle |e[k]| \rangle \simeq e^{j\phi} u^{(r)}[k] \tag{26}$$

in which ϕ is the phase of the unknown scale factor in $e[k]$.

An observation is that both $\mathbf{a}(\widehat{\theta}^{(r)})$ and $\widehat{\boldsymbol{a}}^{(r)}$ are estimates or approximations of the same steering vector $\mathbf{a}(\theta^{(r)})$ except for a complex scale factor, where $\widehat{\theta}^{(r)}$ is a DOA estimate of $\theta^{(r)}$. Therefore, a "blind performance index" is suggested to verify the consistency between $\mathbf{a}(\widehat{\theta}^{(r)})$ and $\widehat{\boldsymbol{a}}^{(r)}$ as follows:

$$\rho(\mathbf{a}(\widehat{\theta}^{(r)}), \widehat{\boldsymbol{a}}^{(r)}) = \frac{|\mathbf{a}^{\mathrm{H}}(\widehat{\theta}^{(r)})\widehat{\boldsymbol{a}}^{(r)}|}{\|\mathbf{a}(\widehat{\theta}^{(r)})\| \cdot \|\widehat{\boldsymbol{a}}^{(r)}\|} \tag{27}$$

which is nothing but the magnitude of the normalized cross-correlation between $\mathbf{a}(\widehat{\theta}^{(r)})$ and $\widehat{\boldsymbol{a}}^{(r)}$ and $0 \leq \rho(\mathbf{a}(\widehat{\theta}^{(r)}), \widehat{\boldsymbol{a}}^{(r)}) \leq 1$. The following remark can be inferred straightforwardly:

(R3) The better the estimation accuracy of both $\widehat{\theta}^{(r)}$ and $\widehat{\boldsymbol{a}}^{(r)}$ (i.e., the better performance of the associated blind beamformer), the larger the value of $\rho(\mathbf{a}(\widehat{\theta}^{(r)}), \widehat{\boldsymbol{a}}^{(r)})$ (or the higher consistency between the two estimates $\mathbf{a}(\widehat{\theta}^{(r)})$ and $\widehat{\boldsymbol{a}}^{(r)}$).

Next, let us present the source extraction scheme that involves the Fourier beamformer and the kurtosis maximization beamformer (KMBF) both based on subcarrier averaging over one OFDM block.

A. Fourier Beamformer by Subcarrier Averaging

The Fourier beamformer by subcarrier averaging is given by

$$\boldsymbol{v}_{\mathrm{FB}} = \frac{1}{\sqrt{Q}} \mathbf{a}(\widetilde{\theta}), \tag{28}$$

where

$$\widetilde{\theta} = \arg \max_{|\theta| \leq \pi/2} \langle | \frac{1}{\sqrt{Q}} \mathbf{a}^{\mathrm{H}}(\theta) \boldsymbol{x}[k]|^2 \rangle \tag{29}$$

is a DOA estimate of $\theta^{(r)}$. Under the assumptions (A1) through (A3) and the noise-free assumption, it can be easily shown, by (20), that

$$\widetilde{\theta} \xrightarrow{\mathrm{p}} \theta^{(r)} \tag{30}$$

for sufficiently large Q where $r \in \{1, 2, ..., L\}$. Therefore, the $\widetilde{\theta}$ given by (29) can be thought of as a DOA estimate, say $\widehat{\theta}^{(r)}$, associated with one source of $\boldsymbol{u}[k]$ (usually the one with the largest path gain) as both Q and N are finite. Note that the above beamformer is similar to the conventional Fourier beamformer [9] but operating in the subcarrier domain. As $\widetilde{\theta} = \theta^{(r)}$ (i.e., one DOA is known in advance), the Fourier beamformer can efficiently extract one source signal $u^{(r)}[k]$ from $\boldsymbol{x}[k]$ (see (14)), and the associated beamformer output given by (22) with $\boldsymbol{v}$ replaced by $\boldsymbol{v}_{\mathrm{FB}}$ is given by

$$e_{\mathrm{FB}}[k] = \boldsymbol{v}_{\mathrm{FB}}^{\mathrm{H}} \boldsymbol{x}[k]. \tag{31}$$

Then the associated channel estimate $\widehat{\boldsymbol{a}}_{\mathrm{FB}}$ can be obtained by (25) and (26) with $\widetilde{e}[k]$ replaced by $\widetilde{e}_{\mathrm{FB}}[k] = e_{\mathrm{FB}}[k]/\langle |e_{\mathrm{FB}}[k]| \rangle$ as

$$\widehat{\boldsymbol{a}}_{\mathrm{FB}} = \langle \boldsymbol{x}[k] \widetilde{e}_{\mathrm{FB}}^{*}[k] \rangle, \tag{32}$$

and the corresponding blind performance index is

$$\rho_{\mathrm{FB}} = \rho(\mathbf{a}(\widetilde{\theta}), \widehat{\boldsymbol{a}}_{\mathrm{FB}}). \quad \text{(by (27))} \tag{33}$$

B. KMBF by Subcarrier Averaging

As the Fourier beamformer cannot completely suppress the strong interfering signals, we present the KMBF by subcarrier averaging that does have this interference suppression feature. Let us first define the kurtosis of $u^{(i)}[k]$ in the subcarrier domain as

$$\gamma\{u^{(i)}[k]\} = \langle |u^{(i)}[k]|^4 \rangle - 2(\langle |u^{(i)}[k]|^2 \rangle)^2 - |\langle (u^{(i)}[k])^2 \rangle|^2, \tag{34}$$

which is a function of $u^{(i)}[k]$ over all the subcarriers. It can be easily shown, by (19) and (34), that

$$\gamma\{u^{(i)}[k]\} \xrightarrow{\mathrm{p}} \eta^{(i)} = -1, \quad \forall\ i. \tag{35}$$

Note that $\eta^{(i)}$ may depend on i for users' symbol sequences rather than QPSK symbol sequences.

The objective function to be maximized for the design of the beamformer $\boldsymbol{v}$ (a $Q \times 1$ vector) is defined as

$$J(\boldsymbol{v}) = J(e[k]) = \frac{|\gamma\{e[k]\}|}{(\langle |e[k]|^2 \rangle)^2} \tag{36}$$

which is also called the "magnitude of normalized kurtosis of $e[k]$" where $e[k]$ is given by (22). Note that the subcarrier averages in $J(\boldsymbol{v})$ given by (36) correspond to the ensemble averages in the conventional "magnitude of normalized kurtosis of $e[k]$" [18]–[20], [24]–[27]. The performance of the optimum beamformer $\boldsymbol{v}$, denoted $\boldsymbol{v}_{\mathrm{KMBF}}$, by maximizing $J(\boldsymbol{v})$ (see (36)) is supported by Theorem 1 below under the noise-free assumption, the preceding three assumptions (A1) through (A3), and the following three assumptions:

(A5) $\tau_{p,j} \neq (\tau_{p,i} + \tau_{p,l})/2$, $\forall\ p$, if $L_p \geq 3$, where i, j, l are distinct integers.

(A6) $\tau_{p,i} + \tau_{p,l} \neq \tau_{p,j} + \tau_{p,m}$, $\forall\ p$, if $L_p \geq 4$, where i, j, l, m are distinct integers.

(A7) $|\tau_{p,j} - \tau_{p,i}| \neq |\tau_{q,m} - \tau_{q,l}|$, $\forall\ p \neq q$, $j \neq i$, and $m \neq l$, if $L_p \geq 2$ and $L_q \geq 2$.

Moreover, the following lemma is needed for the proof of Theorem 1 and the proof of this lemma is given in Appendix C.

Lemma 3. *Under the assumptions (A1) through (A3), (A5) through (A7), and the noise-free assumption,*

$$\langle |e[k]|^2 \rangle \xrightarrow{\mathrm{p}} \sum_{i=1}^{L} |g^{(i)}|^2 \qquad (\text{as } N \to \infty), \tag{37}$$

$$\gamma\{e[k]\} \xrightarrow{\mathrm{p}} \sum_{i=1}^{L} \eta^{(i)} |g^{(i)}|^4 = -\sum_{i=1}^{L} |g^{(i)}|^4 \qquad (\text{as } N \to \infty). \tag{38}$$

Theorem 1. *Under the assumptions (A1) through (A3), (A5) through (A7), and the noise-free assumption,* $J(\boldsymbol{v}_{\mathrm{KMBF}}) = \max\{J(\boldsymbol{v})\} \xrightarrow{\mathrm{p}} 1$, $\boldsymbol{v}_{\mathrm{KMBF}} \xrightarrow{\mathrm{p}} \boldsymbol{v}_{\mathrm{opt}}$, *and* $\boldsymbol{v}_{\mathrm{opt}}^{\mathrm{H}} \boldsymbol{x}[k] = \beta^{(r)} u^{(r)}[k]$ *where* $\beta^{(r)} \neq 0$ *is an unknown constant and* $r \in \{1, ..., L\}$ *is an unknown integer.*

The proof of Theorem 1 is presented in Appendix D. Although the objective function $J(\boldsymbol{v})$ given by (36) is a highly nonlinear function of $\boldsymbol{v}$ without closed-form solutions, fortunately, $\boldsymbol{v}_{\mathrm{KMBF}}$ can be obtained iteratively in the same fashion as the FKMA proposed by Chi *et al.* [18]–[20]. The resultant algorithm is referred to as the *KMBF by subcarrier averaging*. Given $\boldsymbol{v}_{\rm KMBF}^{(i-1)}$ and $e_{\rm KMBF}^{(i-1)}[k]$ obtained at the $(i-1)$th iteration, $\boldsymbol{v}_{\rm KMBF}^{(i)}$ at the ith iteration is obtained by the proposed KMBF through the following two steps.

Step 1. Update $\boldsymbol{v}_{\rm KMBF}^{(i)}$ by

$$\boldsymbol{v}_{\rm KMBF}^{(i)} = \frac{\mathbf{R}_{\boldsymbol{x}}^{-1}\mathbf{d}^*(e_{\rm KMBF}^{(i-1)}[k], \boldsymbol{x}[k])}{\| \mathbf{R}_{\boldsymbol{x}}^{-1}\mathbf{d}^*(e_{\rm KMBF}^{(i-1)}[k], \boldsymbol{x}[k]) \|}, \tag{39}$$

where

$$\mathbf{R}_{\boldsymbol{x}} = \langle \boldsymbol{x}[k]\boldsymbol{x}^{\rm H}[k]\rangle \tag{40}$$

is the subcarrier average based correlation matrix of $\boldsymbol{x}[k]$ and

$$\mathbf{d}(e[k], \boldsymbol{x}[k]) = \langle |e[k]|^2 e[k]\boldsymbol{x}^*[k]\rangle - 2\langle |e[k]|^2\rangle\langle e[k]\boldsymbol{x}^*[k]\rangle - \langle e^2[k]\rangle\langle e^*[k]\boldsymbol{x}^*[k]\rangle \tag{41}$$

is the subcarrier average based 4th-order cross-cumulant between $e[k]$ and $\boldsymbol{x}[k]$ over all the subcarriers. Then obtain the associated $e_{\rm KMBF}^{(i)}[k]$ by (22).

Step 2. If $J(\boldsymbol{v}_{\rm KMBF}^{(i)}) > J(\boldsymbol{v}_{\rm KMBF}^{(i-1)})$, go to the next iteration; otherwise re-update $\boldsymbol{v}_{\rm KMBF}^{(i)}$ through a gradient type optimization algorithm such that $J(\boldsymbol{v}_{\rm KMBF}^{(i)}) > J(\boldsymbol{v}_{\rm KMBF}^{(i-1)})$ and obtain the associated $e_{\rm KMBF}^{(i)}[k]$.

The proposed KMBF is initialized by the Fourier beamformer (i.e., $\boldsymbol{v}_{\rm KMBF}^{(0)} = \boldsymbol{v}_{\rm FB}$), and its performance is supported by Theorem 1 for infinite N and signal-to-noise ratio (SNR). Because both N and SNR are finite in practice, the source signal extracted by the proposed KMBF is then an estimate of one source signal in $\boldsymbol{u}[k]$ (see (15)) except for an unknown scale factor, i.e.,

$$e_{\rm KMBF}[k] = \widehat{u}^{(r)}[k] \simeq \beta^{(r)}u^{(r)}[k]. \tag{42}$$

Then the associated channel estimate $\widehat{\boldsymbol{a}}_{\rm KMBF}$ can be obtained by (25) and (26) with $\widetilde{e}[k]$ replaced by $\widetilde{e}_{\rm KMBF}[k] = e_{\rm KMBF}[k]/\langle |e_{\rm KMBF}[k]|\rangle$ as

$$\widehat{\boldsymbol{a}}_{\rm KMBF} = \langle \boldsymbol{x}[k]\widetilde{e}_{\rm KMBF}^*[k]\rangle, \tag{43}$$

and the corresponding blind performance index is

$$\rho_{\rm KMBF} = \rho(\mathbf{a}(\widetilde{\theta}), \widehat{\boldsymbol{a}}_{\rm KMBF}). \quad \text{(by (27))} \tag{44}$$

Three remarks for the proposed KMBF by subcarrier averaging are as follows:

(R4) As stated in [20], [24], the conventional FKMA uses the MIMO super-exponential algorithm [28] (Step 1) for fast convergence (basically with super-exponential rate) which usually happens in most of iterations before convergence, and a gradient-type optimization method (Step 2) for the guaranteed convergence. Empirically, we found that the proposed iterative KMBF also shares the fast convergence and guaranteed convergence advantages of the conventional FKMA.

(R5) We should emphasize that all the assumptions for Theorem 1 are sufficient conditions rather than necessary conditions for the proposed KMBF, although it may or may not fail to extract some sources when not all the extra assumptions of (A5), (A6) and (A7) are satisfied while the other assumptions (A1), (A2), and (A3) in Theorem 1 are true. Additionally, the probability of the event that violation of any of the three assumptions occurs depends on values of N_g (length of GI) and L_p (number of paths of each user). However, this drawback can be avoided by combining the KMBF and the Fourier beamformer to be presented in the next subsection.

(R6) The proposed KMBF is also applicable to the case of binary phase-shift keying (BPSK) symbol sequences. For this case, in addition to the noise-free assumption and the assumptions (A1) through (A3) and (A5) to (A7) (required for the case of QPSK symbol sequences), three more assumptions are required as follows:

(A8) $\tau_{q,m} \neq (\tau_{p,i} + \tau_{p,j})/2$, $\forall\ m$, $q \neq p$, and $i \neq j$ if $L_p \geq 2$;

(A9) $\tau_{p,i} + \tau_{p,l} \neq \tau_{q,j} + \tau_{q,m}$, $\forall\ q \neq p$, $i \neq l$, and $j \neq m$, if $L_p \geq 2$ and $L_q \geq 2$;

(A10) $\tau_{p,i} \neq \tau_{q,l}$, $\forall\ i$, l, and $q \neq p$, if $\tau_{p,i} > 0$ and $\tau_{q,l} > 0$;

for Lemma 3 and Theorem 1 to hold valid, and meanwhile

$$\eta^{(i)} = \begin{cases} -2, & \text{as } \tau^{(i)} = 0 \\ -1, & \text{as } \tau^{(i)} \neq 0. \end{cases} \tag{45}$$

(The proof of Lemma 3 and Theorem 1 for the BPSK case is similar to that for the QPSK case and thus omitted here.) Therefore, the proposed KMBF may fail to extract a source with a higher probability for the BPSK case than for the QPSK case (see (R5)) due to the above three extra assumptions required, implying that the Fourier beamformer may perform better than the KMBF, though both of them are based on subcarrier averaging for the BPSK case.

C. Fourier-KMBF by Subcarrier Averaging

We empirically found that the KMBF performs better than the Fourier beamformer (both based on subcarrier averaging), but the former requires three extra assumptions (A5), (A6) and (A7). It may occur that while the assumption (A2) holds, these three assumptions may not be valid all the time in practice, thus limiting the performance of the KMBF. This motivates the following two-step hybrid Fourier-KMBF which is free from these three assumptions:

(S1) Obtain the beamformer output $e[k]$, channel estimate $\widehat{\boldsymbol{a}}$, and blind performance ρ of both the Fourier beamformer and the KMBF presented in Section 3.1 and Section 3.2, respectively.

(S2) Let $\rho_{\max} = \max\{\rho_{\rm FB}, \rho_{\rm KMBF}\}$. If $\rho_{\max} > \eta_d$ where η_d is a preassigned threshold, then obtain the extracted source and the channel estimate

$$(e[k], \widehat{\boldsymbol{a}}) = \begin{cases} (e_{\rm KMBF}[k], \widehat{\boldsymbol{a}}_{\rm KMBF}), & \text{if } \rho_{\max} = \rho_{\rm KMBF} \\ (e_{\rm FB}[k], \widehat{\boldsymbol{a}}_{\rm FB}), & \text{if } \rho_{\max} = \rho_{\rm FB}, \end{cases} \tag{46}$$

otherwise no more source signal (with enough power) can be extracted.

A remark about the proposed hybrid Fourier-KMBF is as follows:

(R7) Again, when not all the extra assumptions needed for the corresponding modulation (i.e., QPSK or BPSK)

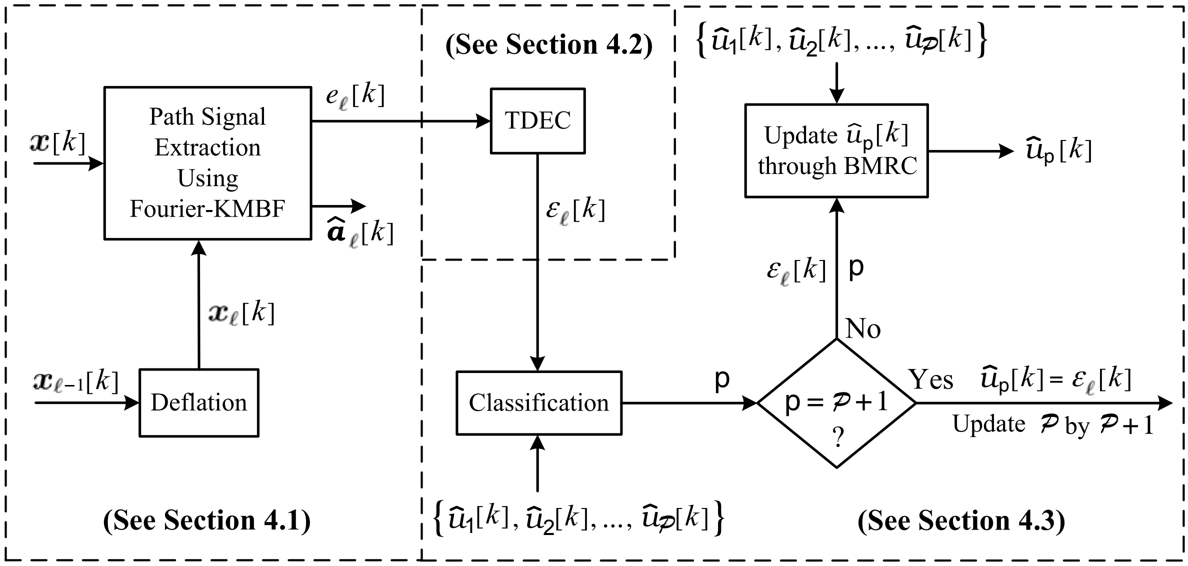

Fig. 2. Signal processing procedure of the proposed blind MSBFA at stage ℓth.

are satisfied while the other assumptions in Theorem 1 are true, the selection scheme (46) will switch to the Fourier beamformer since $\rho_{\mathrm{FB}} > \rho_{\mathrm{KMBF}}$ in this case, indicating that the proposed hybrid Fourier-KMBF is an intelligent selection scheme according to the performance of the Fourier beamformer and the KMBF (see (R3)). Therefore, all the extra assumptions (A5) through (A10) can be removed.

IV. Proposed Blind MSBFA

Under Assumptions (A1) through (A4), the proposed blind MSBFA as shown in Figure 2 basically includes path signal extraction (i.e., source extraction), time delay estimation and compensation, classification (path-to-user association) and BMRC (of paths) which are presented next, respectively. We also discuss the applicability of the proposed algorithm when correlated paths are present.

A. Multistage Path Signal Extraction Using Fourier-KMBF

Assume that the path signal estimate $e_{\ell-1}[k]$ and the channel estimate $\widehat{\boldsymbol{a}}_{\ell-1}$ are obtained at stage $\ell-1$ and that $\boldsymbol{x}_\ell[k]$ is the MIMO signal deflated from $\boldsymbol{x}[k]$ at stage ℓ (i.e., all the contributions of the extracted path signals up to stage $\ell-1$ removed). As shown in Figure 2, at stage ℓ,

$$\boldsymbol{x}_\ell[k] = \boldsymbol{x}_{\ell-1}[k] - \widehat{\boldsymbol{a}}_{\ell-1} e_{\ell-1}[k]. \quad (47)$$

First, obtain a distinct DOA estimate $\widetilde{\theta} = \widehat{\theta}^{(r)}$ by (29) with $\boldsymbol{x}[k]$ replaced by $\boldsymbol{x}_\ell[k]$, and then calculate $\boldsymbol{v}_{\mathrm{FB}}^{(\ell)}$ by (28). Second, obtain $(e_\ell[k], \widehat{\boldsymbol{a}}_\ell)$ using the proposed Fourier-KMBF (see (46)), where

$$e_\ell[k] = \widehat{u}^{(r)}[k] \simeq \beta_\ell u_p[k] e^{-j2\pi k \tau^{(r)}/N} \quad \text{(by (17))} \quad (48)$$

in which β_ℓ is an unknown constant, $r \in \{1, ..., L\}$ is unknown and r maps uniquely to a "user p" (by (21)). Note that the extracted path signal $e_\ell[k]$ is basically free from error propagation from stage to stage [19]–[22] since $\boldsymbol{x}[k]$ instead of $\boldsymbol{x}_\ell[k]$ is processed by the Fourier-KMBF at each stage.

B. Time Delay Estimation and Compensation (TDEC)

The unknown time delay $\tau^{(r)}$ in the extracted path signal $e_\ell[k]$ (see (48)) can be estimated by subcarrier averaging as

$$\widehat{\tau}^{(r)} = \arg \max_{0 \le \tau \le N_g} |\langle (\widetilde{e}_\ell[k] e^{j2\pi k\tau/N})^4 \rangle| \quad (49)$$

simply because $|\langle (\widetilde{e}_\ell[k] e^{j2\pi k\tau/N})^4 \rangle| \simeq 0$ for $\tau \neq \tau^{(r)}$, while $|\langle (\widetilde{e}_\ell[k] e^{j2\pi k\tau^{(r)}/N})^4 \rangle| \simeq 1$. Therefore, by (48) and (49), the time delay compensated path signal estimate can be obtained in a straightforward manner as

$$\varepsilon_\ell[k] = e_\ell[k] e^{j2\pi k \widehat{\tau}^{(r)}/N} = \beta_\ell u_p[k] + \varpi_\ell[k], \quad (50)$$

where β_ℓ is an unknown constant, the user $p \in \{1, 2, ..., P\}$ is also unknown since r is unknown, and $\varpi_\ell[k]$ is the estimation error.

C. Classification and BMRC

Assume that at stage $\ell - 1$, the time delay compensated path signal estimates $\{\varepsilon_1[k], \varepsilon_2[k], ..., \varepsilon_{\ell-1}[k]\}$ (see (50)) have been optimally combined into a set of $\mathcal{P}$ symbol estimates, $\mathcal{S} = \{\widehat{u}_q[k], q = 1, 2, ..., \mathcal{P}\}$ where the subscript 'q' is merely a "class number" (associated with a distinct user number) but not the actual user number because the implicit user number p associated with the extracted path signal $\varepsilon_\ell[k]$ is unknown. Therefore, it is needed to identify the association pair of $\widehat{u}_q[k]$ and $\varepsilon_\ell[k]$ so that $\widehat{u}_q[k]$ can be updated through BMRC processing.

Next, let ϱ_q denote the magnitude of normalized cross-correlation by subcarrier averaging between $\varepsilon_\ell[k]$ and $\widehat{u}_q[k]$ defined as

$$\varrho_q = \frac{|\langle \varepsilon_\ell[k] \widehat{u}_q^*[k] \rangle|}{\sqrt{\langle |\varepsilon_\ell[k]|^2 \rangle \langle |\widehat{u}_q[k]|^2 \rangle}} \quad (51)$$

$(0 \le \varrho_q \le 1)$ and let

$$\mathsf{p} = \arg \max_{1 \le q \le \mathcal{P}} \{\varrho_q\}. \quad (52)$$

As shown in Figure 2, if $\varrho_{\mathsf{p}} < \eta_c$ (a preassigned threshold), $\varepsilon_\ell[k]$ is classified as a member of a new class and then set $\mathsf{p} = \mathcal{P}+1$ and $\widehat{u}_{\mathsf{p}}[k] = \varepsilon_\ell[k]$, and update $\mathcal{P}$ by $\mathcal{P}+1$; otherwise $\varepsilon_\ell[k]$ is classified as a member of the existent class p and update $\widehat{u}_{\mathsf{p}}[k]$ by BMRC using the FKMA proposed by Chi *et al.* [18]–[22], where the BMRC of $\widehat{u}_{\mathsf{p}}[k]$ and $\varepsilon_\ell[k]$ (which is a coherent combination of $\widehat{u}_{\mathsf{p}}[k]$ and $\varepsilon_\ell[k]$) can increase the diversity gain of the updated $\widehat{u}_{\mathsf{p}}[k]$ maximally.

D. Applicability of MSBFA in the Presence of Correlated Paths

In this subsection, we discuss the applicability of the proposed algorithm when either the assumption (A3) or the assumption (A2) can be partly relaxed. In practice, path signals from different DOAs that belong to the same user may impinge on the receiver antenna array at the same time (i.e, with the same time delay), forming a "cluster" of spatially correlated path signals [9], [14], [15] and thus violating Assumption (A3); path signals with different time delays that belong to the same user may impinge on the receiver antenna array from the same DOA, forming a "cluster" of temporally correlated path signals and thus violating Assumption (A2). For the case of the presence of spatially correlated paths, the proposed MSBFA is applicable. The reasons are as follows.

Assume that $\{\alpha_{p,l}^{(m)}\mathbf{a}(\theta_{p,l}^{(m)})s_p[n-\tau_{p,l}], m = 1,2,...,L_{p,l}\}$ is a cluster of $L_{p,l}$ spatially correlated path signals impinging on the receiver antenna array where $\alpha_{p,l}^{(m)}$ and $\theta_{p,l}^{(m)}$ are the path gain and DOA of each correlated signal in the cluster, respectively. The received signal $\mathbf{x}[n]$ given by (2) remains valid except that $\alpha_{p,l}\mathbf{a}(\theta_{p,l})$ must be replaced by

$$\bar{\boldsymbol{a}}_{p,l} = \sum_{m=1}^{L_{p,l}} \alpha_{p,l}^{(m)}\mathbf{a}(\theta_{p,l}^{(m)}). \tag{53}$$

The resultant MIMO signal model for the post-FFT BFS given by (14) (on which the proposed MSBFA is based) also keeps valid except that the mixing matrix $\mathbf{A}$ is different due to the replacement of $\alpha_{p,l}\mathbf{a}(\theta_{p,l})$ by $\bar{\boldsymbol{a}}_{p,l}$. Therefore, the proposed MSBFA is able to effectively estimate the associated source signal $u_{p,l}[k] = u_p[k]e^{-j2\pi k\tau_{p,l}/N}$ as long as $\|\bar{\boldsymbol{a}}_{p,l}\|$ is large enough, implying its robustness to spatially correlated paths. On the other hand, the Capon's MV beamformer is incapable of extracting the associated source $s_p[n-\tau_{p,l}]$ regardless of the value of $\|\bar{\boldsymbol{a}}_{p,l}\|$ because $\bar{\boldsymbol{a}}_{p,l}$ is no longer a steering vector of a certain DOA required by the Capon's MV beamformer [9], [11]–[15].

For the case of the presence of temporally correlated paths with the same DOA, an example is that one non-integer-delayed path will lead to two (or more) consecutive integer-delayed paths in discrete-time domain after sampling, i.e., $\tau_{p,l+1} = \tau_{p,l}+1$ (for two consecutive integer delays), which will result in a combined path signal $u'_{p,l}[k] = u_{p,l}[k] + u_{p,l+1}[k] = u_{p,l}[k](a + be^{-j2\pi k/N})$ (where a and b are constants) incident upon the receiver antenna array from the same DOA. Though $|\tau_{p,l+1} - \tau_{p,l}| = 1$ may happen in two different users, it is totally different from the case that (A7) is not satisfied but (A1) through (A3) are satisfied as mentioned in (R5) simply due to the same DOA of the two paths. The extraction and TDEC of this type of path signals need further rigorous theoretical support though we have done some promising preliminary studies which will be reported in the future due to space limit.

V. Simulation Results

Two simulation examples are to be presented to justify the effectiveness of the proposed MSBFA. Example 1 considers the case of no correlated paths and Example 2 considers the case of the presence of spatially correlated paths. Consider a four-user ($P = 4$) OFDM system with FFT size $N = 1024$, length of GI $N_g = 20$, and antenna array size $Q = 20$. The synthetic MIMO signals $\mathbf{x}[n]$ were generated by (4) for users' symbol sequences $u_p[k]$'s being i.i.d. BPSK or QPSK signals with $E\{|u_p[k]|^2\} = 1$ and the noise vector $\mathbf{w}[n]$ being i.i.d. zero-mean Gaussian with $E\{\mathbf{w}[n]\mathbf{w}^{\mathrm{H}}[n]\} = \sigma_w^2\mathbf{I}_Q$. Then the proposed MSBFA with the thresholds $\eta_d = 0.75$ and $\eta_c = 0.5$ was employed to process the associated MIMO signal $\boldsymbol{x}[k]$ (see (14)) to estimate all the four users' symbol sequences $u_p[k]$'s. For performance comparison, the same data (either pre-FFT data $\mathbf{x}[n]$ or post-FFT data $\boldsymbol{x}[k]$) were processed by theoretical nonblind MMSE and MRC beamformers as well as Capon's MV beamformer. Twenty five hundred independent runs were performed for different values of input SNR, defined as

$$\text{Input SNR} = \frac{E\{\|\mathbf{x}[n]-\mathbf{w}[n]\|^2\}}{P\cdot E\{\|\mathbf{w}[n]\|^2\}}. \quad \text{(see (4))}$$

The performance of each beamformer under test is evaluated in terms of the averaged symbol error rate (SER) of all the users' symbol estimates. Next, let us concentrate on Example 1.

Example 1. (Environment without Correlated Paths)

All the multipath channel parameters (except time delay parameters) used in this example are shown in Table 1. Note that $\sum_{l=1}^{L_p}|\alpha_{p,l}|^2 = 1$. Fifty sets of time delay parameters $\tau_{p,l} \in \{0,1,...,N_g\}$, for $p = 1,2,...,P$ and $l = 1,2,...,L_p$, were generated randomly. For each set of time delay parameters, fifty sets of data $\mathbf{x}[n]$ were generated.

In order to give insights into the performance of the proposed blind MSBFA, Figures 3(a) (for the QPSK case) and 3(b) (for the BPSK case) show the performance (averaged SER) of the proposed MSBFA without BMRC (dashed lines), where either the the Fourier beamformer (Section 3.1), or the KMBF (Section 3.2), or the Fourier-KMBF (Section 3.3) was used in the source (path signal) extraction. In addition, the performance of the proposed blind MSBFA with BMRC is also presented (solid lines) where the Fourier-KMBF was used in the source extraction. One can observe, from Figure 3(a), that the proposed MSBFA without BMRC (dashed line) performs best when the Fourier-KMBF (◯) is used, and that the proposed MSBFA with BMRC (◯ and solid line) performs much better than the one without BMRC (◯ and dashed line). The same observations from Figure 3(a) can also be applied to Figure 3(b). Moreover, it is worth mentioning that the proposed MSBFA without BMRC (dashed line) using the KMBF (□) performs better than using the Fourier beamformer (△) for the QPSK case (see Figure 3(a)), while for the BPSK

TABLE I
MULTIPATH CHANNEL PARAMETERS USED IN EXAMPLE 1 INCLUDING PATH GAINS AND DOAS.

Path Number (l)	User 1 ($L_1 = 4$)		User 2 ($L_2 = 2$)		User 3 ($L_3 = 2$)		User 4 ($L_4 = 2$)	
	$\alpha_{1,l}$	$\theta_{1,l}$	$\alpha_{2,l}$	$\theta_{2,l}$	$\alpha_{3,l}$	$\theta_{3,l}$	$\alpha_{4,l}$	$\theta_{4,l}$
1	0.5442	45°	0.7634	-60°	0.8682	-45°	0.8944	60°
2	0.5140	-30°	0.6459	80°	0.4961	35°	0.4472	-10°
3	0.4837	20°	—	—	—	—	—	—
4	0.4535	0°	—	—	—	—	—	—

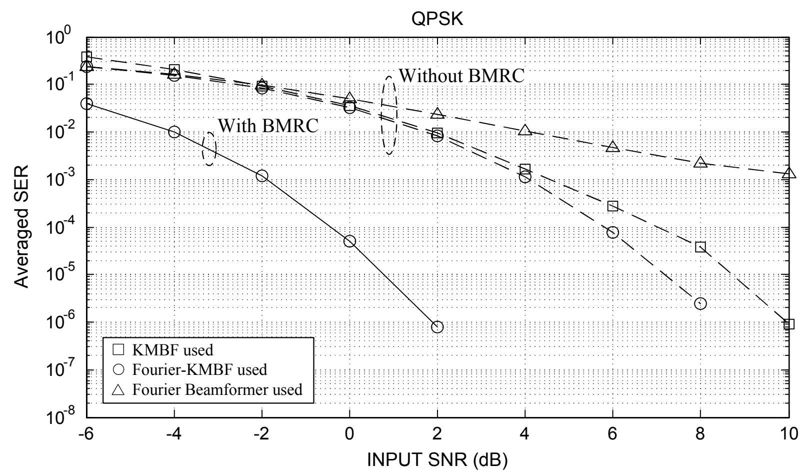

(a)

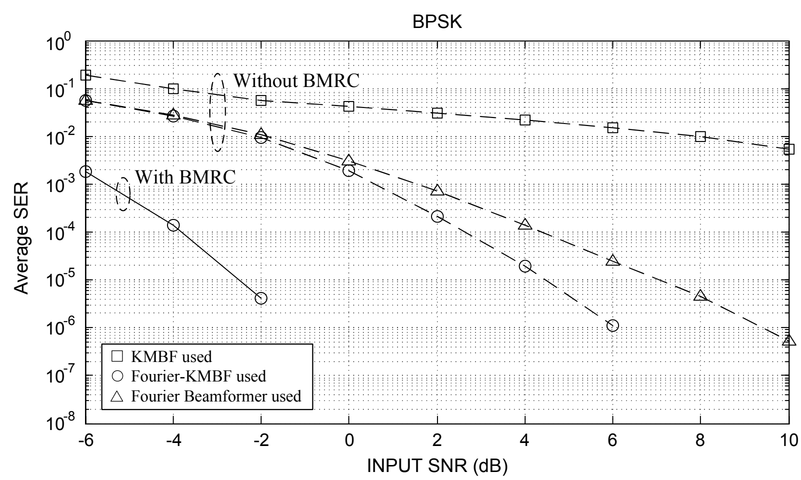

(b)

Fig. 3. Performance (averaged SER) of the proposed blind MSBFA (solid lines for BMRC included and dash lines for BMRC excluded) for (a) QPSK case and (b) BPSK case, with no correlated paths.

case (see Figure 3(b)) the situation is just the contrary. These results are consistent with (R6).

Next, some simulation results using the MSBFA, nonblind MMSE and MRC beamformers associated with the pre-FFT BFS or post-FFT BFS, and Capon's MV beamformer associated with the pre-FFT BFS are shown in Figure 4(a) for the QPSK case and in Figure 4(b) for the BPSK case. One can observe, from Figure 4(a), that the MSBFA (◯ and solid line), nonblind MMSE (△ and solid line) and MRC beamformers (□ and solid line) associated with the post-FFT BFS significantly outperform the other beamformers associated with the pre-FFT BFS including nonblind MMSE (△ and dash line) and MRC beamformers (□ and dash line), theoretic Capon's MV beamformer (◊ and dash line) (using theoretical correlation matrix and true DOAs) and actual Capon's MV beamformer (▽ and dash line) (using the estimated correlation matrix and estimated DOAs) because path diversity gain exists only for the former (see (R1)). Note that the performance of the theoretic Capon's MV beamformer is actually the same as the nonblind MMSE beamformer associated with the pre-FFT BFS (dash line) and they perform better than the actual Capon's MV beamformer. Moreover, the proposed MSBFA works well with better performance than the nonblind MRC beamformer associated with the post-FFT BFS, although the

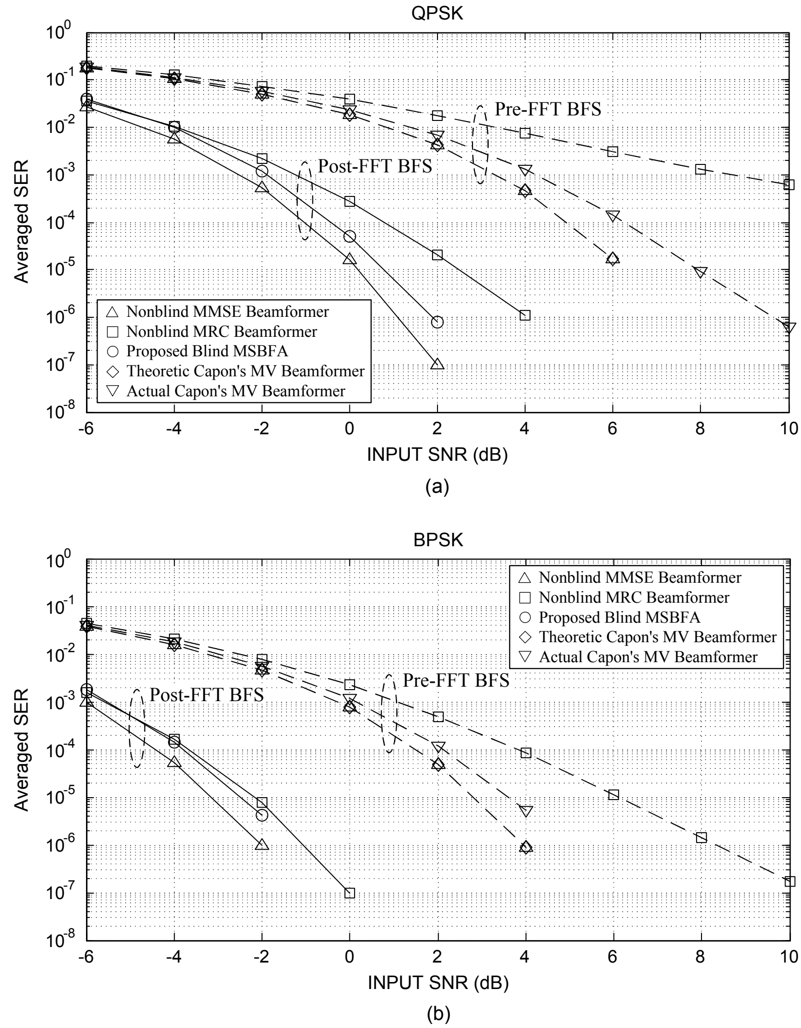

Fig. 4. Performance (averaged SER) of beamformers under test associated with the pre-FFT BFS (dash lines) and those associated with the post-FFT BFS (solid lines), for (a) QPSK case and (b) BPSK case, with no correlated paths.

performance of the former is slightly worse than that of the nonblind MMSE beamformer associated with the post-FFT BFS. The observations of Figure 4(a) also apply to Figure 4(b).

Example 2. (Environment with Spatially Correlated Paths) All the channel parameters used in Example 1 are basically used in this example, except that each path with DOA $\theta_{p,l}$ and path gain $\alpha_{p,l}$ is replaced by a cluster of $L_{p,l} = 4$ spatially correlated paths with distinct DOAs $\theta_{p,l}^{(m)}$ ($|\theta_{p,l}^{(m)} - \theta_{p,l}^{(1)}| \leq 5°$) and path gains $\alpha_{p,l}^{(m)} \ll \alpha_{p,l}^{(1)}$, $m = 2, 3, ..., L_{p,l}$, and $\sum_{l=1}^{L_p} |\alpha_{p,l}^{(1)}|^2 = 1$.

The simulation results corresponding to Figure 4 (for the case of no correlated paths) are shown in Figure 5 for the case of spatially correlated paths. Basically, all the observations from Figures 4(a) (for the QPSK case) and 4(b) (for the BPSK case) apply to Figure 5(a) (for the QPSK case) and 5(b) (for the BPSK case), respectively, i.e., beamformers associated with the post-FFT BFS outperform those associated with the pre-FFT BFS, and the proposed MSBFA works well and outperforms the nonblind MRC beamformer associated with the post-FFT BFS, but it performs slightly worse than the nonblind MMSE beamformer associated with the post-FFT BFS. Besides, all the beamformers under test perform better for higher input SNR except the Capon's MV beamformer (either theoretical one or actual one), which performs worse (better) for higher input SNR as input SNR is higher (lower) than 4 dB, demonstrating that it is not applicable in the presence of spatially correlated paths.

The above simulation examples demonstrate the efficacy of the proposed blind MSBFA, in spite of no comparison with other block-by-block post-FFT beamforming algorithms for multiuser OFDM systems since, to our best knowledge, so far none of them can be found in the open literature.

VI. Conclusion

We have presented a block-by-block post-FFT beamforming algorithm based on subcarrier averaging, namely the blind MSBFA, which is well suited to outdoor rural environments with some but not too many multiple paths, for the data sequence estimation of a multiuser OFDM system. It is also a multistage blind beamforming algorithm (without involving user identification) consisting of path signal extraction using

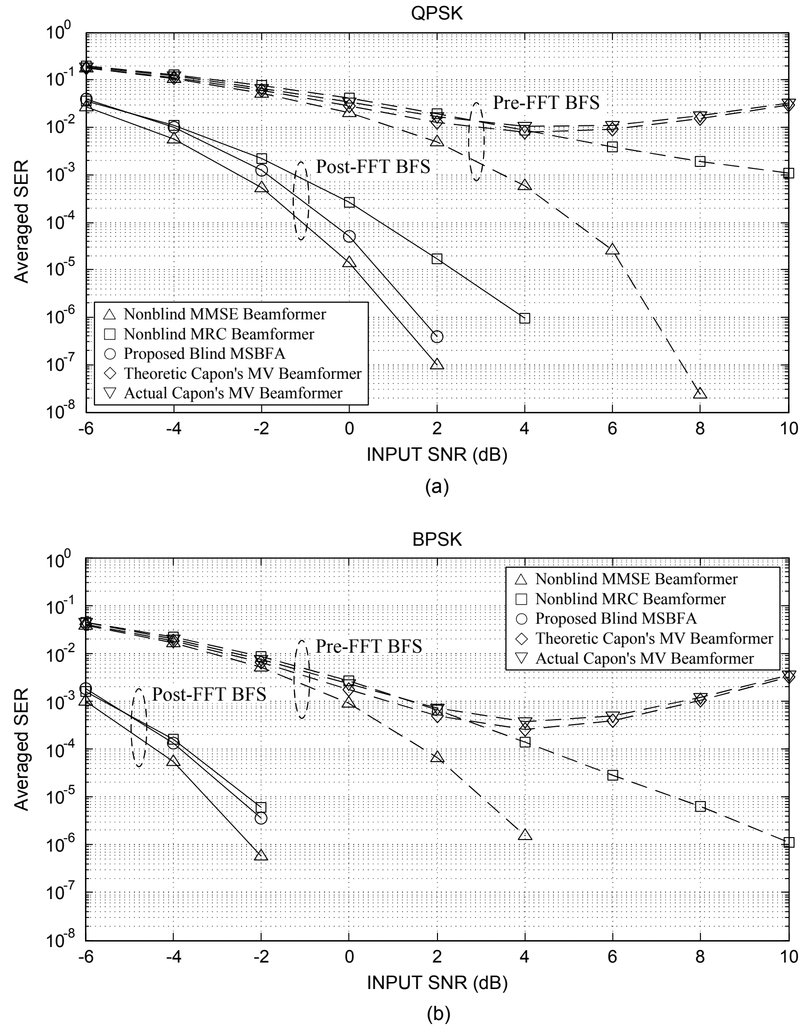

Fig. 5. Performance (averaged SER) of beamformers under test associated with the pre-FFT BFS (dash lines) and those associated with the post-FFT BFS (solid lines), for (a) QPSK case and (b) BPSK case, with spatially correlated paths.

the proposed blind Fourier-KMBF, TDEC processing, classification and BMRC processing at each stage as shown in Figure 2. Note that the blind Fourier-KMBF used by the proposed MSBFA is also an automatic selection scheme according to the performance of two blind beamformers, the KMBF and the Fourier beamformer, both using subcarrier averages over one OFDM block. Moreover, like the conventional FKMA, the KMBF by subcarrier averaging supported by Theorem 1 is also a computationally fast source extraction algorithm. Our simulation results demostrate that the proposed MSBFA performs well no matter whether spatially correlated paths (resultant from the same arrival time of path signals from distinct DOAs) are present or not, and its performance is close to the "optimal" nonblind MMSE beamformer associated with the post-FFT BFS. The applicability of the proposed MSBFA in the presence of temporally correlated paths with the same DOA is currently being investigated.

Appendix

A. Proof of Lemma 1

Assume that $u^{(l)}[k] = u_p[k]e^{-j2\pi\tau^{(l)}k/N}$ and $u^{(m)}[k] = u_q[k]e^{-j2\pi\tau^{(m)}k/N}$ (see (17) and (21)) are associated with users p and q, respectively. By (18) and Assumptions (A1) and (A3), it can be easily shown that

$$E\{\langle(u^{(l)}[k])^2\rangle\} = \frac{1}{N}\sum_{k=0}^{N-1} E\{u_p^2[k]\}e^{-j4\pi\tau^{(l)}k/N} = 0 \quad (\text{since } E\{u_p^2[k]\} = 0), \tag{54}$$

$$E\{\langle u^{(m)}[k](u^{(l)}[k])^*\rangle\} = \frac{1}{N}\sum_{k=0}^{N-1} E\{u_q[k]u_p^*[k]\}e^{-j2\pi(\tau^{(m)}-\tau^{(l)})k/N} = 0 \tag{55}$$

(where in obtaining (55), we have used the facts that $\tau^{(m)} \neq \tau^{(l)}$ for $m \neq l$ and $q = p$, and that $u_p[k]$ and $u_q[k]$ are zero-mean statistically independent random variables for $q \neq p$),

$$
\begin{aligned}
E\{|\langle (u^{(l)}[k])^2\rangle|^2\} &= E\{|\frac{1}{N}\sum_{k=0}^{N-1}(u^{(l)}[k])^2|^2\} \\
&= E\{\frac{1}{N^2}\sum_{k_1=0}^{N-1}\sum_{k_2=0}^{N-1}(u^{(l)}[k_1])^2((u^{(l)}[k_2])^*)^2\} \\
&= \frac{1}{N^2}\sum_{k_1=0}^{N-1}E\{|u^{(l)}[k_1]|^4\} \\
&\quad + \frac{1}{N^2}\sum_{k_1=0}^{N-1}\sum_{k_2\neq k_1}^{N-1}E\{(u^{(l)}[k_1])^2((u^{(l)}[k_2])^*)^2\} \\
&= \frac{1}{N} \\
&\quad + \frac{1}{N^2}\sum_{k_1=0}^{N-1}\sum_{k_2\neq k_1}^{N-1}E\{u_p^2[k_1]\}E\{(u_p^*[k_2])^2\}e^{-j\frac{4\pi}{N}\tau^{(l)}(k_1-k_2)} \\
&= \frac{1}{N} \quad (\text{since } E\{u_p^2[k]\}=0),
\end{aligned} \tag{56}
$$

and

$$
\begin{aligned}
E\{|\langle u^{(m)}[k](u^{(l)}[k])^*\rangle|^2\} &= E\{|\frac{1}{N}\sum_{k=0}^{N-1}u^{(m)}[k](u^{(l)}[k])^*|^2\} \\
&= E\{\frac{1}{N^2}\sum_{k_1=0}^{N-1}\sum_{k_2=0}^{N-1}u^{(m)}[k_1](u^{(l)}[k_1])^*(u^{(m)}[k_2])^*u^{(l)}[k_2]\} \\
&= \frac{1}{N^2}\sum_{k_1=0}^{N-1}E\{|u^{(m)}[k_1]|^2|u^{(l)}[k_1]|^2\} \\
&\quad + \frac{1}{N^2}\sum_{k_1=0}^{N-1}\sum_{k_2\neq k_1}^{N-1}E\{u^{(m)}[k_1](u^{(l)}[k_1])^*(u^{(m)}[k_2])^*u^{(l)}[k_2]\} \\
&= \frac{1}{N^2}\sum_{k_1=0}^{N-1}E\{|u_p[k_1]|^2|u_q[k_1]|^2\} \\
&\quad + \frac{1}{N^2}\sum_{k_1=0}^{N-1}\sum_{k_2\neq k_1}^{N-1}E\{u_q[k_1]u_p^*[k_1]u_q^*[k_2]u_p[k_2]\} \\
&\quad \cdot e^{-j2\pi(\tau^{(m)}-\tau^{(l)})(k_1-k_2)/N} \\
&= \begin{cases} 1/N, & \text{for } q\neq p \\ 0, & \text{for } q=p, \end{cases}
\end{aligned} \tag{57}
$$

where in obtaining (57), we have used the fact that $\tau^{(m)} \neq \tau^{(l)}$ for $l \neq m$ and $q = p$, and the fact that $u_p[k_1]$, $u_p[k_2]$, $u_q[k_1]$ and $u_q[k_2]$ are zero-mean statistically independent random variables as $k_2 \neq k_1$ for $q \neq p$. Because $E\{|\langle (u^{(l)}[k])^2\rangle|^2\} \to 0$ (by (56)) and $E\{|\langle u^{(m)}[k](u^{(l)}[k])^*\rangle|^2\} \to 0$ (by (57)) as $N \to \infty$, both of $\langle (u^{(l)}[k])^2\rangle$ and $\langle u^{(m)}[k](u^{(l)}[k])^*\rangle$ converge in the mean-square sense to zero as $N \to \infty$. Therefore, we have completed the proof for (19) and (20) since mean-square convergence implies convergence in probability.

B. Proof of Lemma 2

Under the assumptions (A1) through (A3) and the noise-free assumption, and by (14), (5) and (15), it can be easily inferred that

$$
\begin{aligned}
\langle \boldsymbol{x}[k](u^{(r)}[k])^*\rangle &= \langle \sum_{l=1}^{L}\boldsymbol{a}^{(l)}u^{(l)}[k](u^{(r)}[k])^*\rangle \\
&= \sum_{l=1}^{L}\boldsymbol{a}^{(l)}\langle u^{(l)}[k](u^{(r)}[k])^*\rangle \\
&\xrightarrow{\text{p}} \boldsymbol{a}^{(r)} = \alpha^{(r)}\mathbf{a}(\theta^{(r)}). \quad (\text{by } (20))
\end{aligned} \tag{58}
$$

Thus we have completed the proof of Lemma 2.

C. Proof of Lemma 3

Through the same procedure of the proof of Lemma 1, the following subcarrier averages can be shown to converge in probability as $N \to \infty$:

$$\langle u^{(l)}[k]u^{(m)}[k]\rangle \xrightarrow{\text{p}} 0 \tag{59}$$
$$\langle (u^{(l)}[k])^2((u^{(m)}[k])^*)^2\rangle \xrightarrow{\text{p}} 0 \tag{60}$$
$$\langle (u^{(l)}[k])^2(u^{(m)}[k])^*(u^{(i)}[k])^*\rangle \xrightarrow{\text{p}} 0 \tag{61}$$
$$\langle u^{(l)}[k]u^{(m)}[k](u^{(i)}[k])^*(u^{(j)}[k])^*\rangle \xrightarrow{\text{p}} 0 \tag{62}$$

where l, m, i, j are distinct integers. Note that the proofs of (59) and (60) require the assumptions (A1) and (A3), that the proof of (61) requires the assumptions (A1), (A3) and (A5), and that the proof of (62) requires the assumptions (A1), (A3), (A6) and (A7).

With the assumptions (A1) through (A3) and (A5) through (A7), and the noise-free assumption, it can be shown, by (22), (23), and (20), that

$$
\begin{aligned}
\langle |e[k]|^2\rangle &= \sum_{l=1}^{L}|g^{(l)}|^2\langle |u^{(l)}[k]|^2\rangle \\
&\quad + \sum_{l=1}^{L}\sum_{m=1,m\neq l}^{L}g^{(l)}(g^{(m)})^*\langle u^{(l)}[k](u^{(m)}[k])^*\rangle \\
&\xrightarrow{\text{p}} \sum_{l=1}^{L}|g^{(l)}|^2
\end{aligned} \tag{63}
$$

which is exactly (37), and by Lemma 1 and (59) through (62), that

$$\langle |e[k]|^4\rangle - |\langle e^2[k]\rangle|^2 \xrightarrow{\text{p}} \sum_{l=1}^{L}\eta^{(l)}|g^{(l)}|^4 + 2(\sum_{l=1}^{L}|g^{(l)}|^2)^2, \tag{64}$$

as $N \to \infty$ where tedious algebraic derivations in obtaining (64) are omitted here due to limited space. According to (63), (64) and (34), one can infer that

$$\gamma\{e[k]\} \xrightarrow{\text{p}} \sum_{l=1}^{L}\eta^{(l)}|g^{(l)}|^4 = -\sum_{l=1}^{L}|g^{(l)}|^4 \quad (\text{by } (35)) \tag{65}$$

as $N \to \infty$ which is exactly (38). Thus we have completed the proof of Lemma 3.

D. Proof of Theorem 1

Under the assumptions (A1) through (A3), (A5) through (A7), and the noise-free assumption, and by (36), Lemma 3, and the carry-over property of "convergence in probability" as $N \to \infty$, one can easily infer

$$J(e[k]) = J(\mathbf{g}) \xrightarrow{\text{p}} J_{\text{KMA}}(e[k]) = J_{\text{KMA}}(\mathbf{g}) = \frac{|\sum_{l=1}^{L} \eta^{(l)} |g^{(l)}|^4|}{(\sum_{l=1}^{L} |g^{(l)}|^2)^2}. \quad (66)$$

Because of $|\eta^{(l)}| = 1$ for all l by (35), the set of all the local optimum solutions for $\mathbf{g}$ such that $J_{\text{KMA}}(e[k])$ is maximum has been known as $S(\mathbf{g}) = \{\mathbf{g} |\ g^{(l)}\boldsymbol{\zeta}_i,\ i = 1,\ 2, ..., L\}$ where $\boldsymbol{\zeta}_i$ is an $L \times 1$ unit vector with the ith element equal to unity and the other elements equal to zero. In other words,

$$J(e_{\text{KMBF}}[k]) = J(\boldsymbol{v}_{\text{KMBF}}) \xrightarrow{\text{p}} J_{\text{KMA}}(\mathbf{g} = g^{(r)}\boldsymbol{\zeta}_r) = |\eta^{(r)}| = 1 \quad (67)$$

and $\boldsymbol{v}_{\text{KMBF}} \xrightarrow{\text{p}} \boldsymbol{v}_{\text{opt}}$ for which $\boldsymbol{v}_{\text{opt}}^{\text{H}}\boldsymbol{x}[k] = \boldsymbol{v}_{\text{opt}}^{\text{H}}\mathbf{A}\boldsymbol{u}[k] = \mathbf{g}^{\text{T}}\boldsymbol{u}[k] = g^{(r)}\boldsymbol{\zeta}_r^{\text{T}}\boldsymbol{u}[k] = g^{(r)}u^{(r)}[k]$ (i.e., $\beta^{(r)} = g^{(r)}$), where $r \in \{1, 2, ..., L\}$. Thus, we have completed the proof.

ACKNOWLEDGEMENTS

The authors would like to sincerely thank Mr. Chen Xiang and Mr. Cheng-Wei Lin for their helps and suggestions during the preparation and revision of the manuscript.

REFERENCES

[1] M. Budsabathon, Y. Hara, and S. Hara, "Optimum beamforming for pre-FFT OFDM adaptive antenna array," *IEEE Trans. Veh. Technol.*, vol. 53, pp. 945–955, July 2004.

[2] Y. Zeng and T. S. Ng, "A subspace method for channel estimation of multi-user multi-antenna OFDM system," in *Proc. IEEE International Symposium on Circuits and Systems*, vol. 3, Bangkok, Thailand, May 2003, pp. III-52–III-55.

[3] R. V. Nee and R. Prasad, *OFDM for Wireless Multimedia Communications.* Boston: Artech House, 1999.

[4] M. Okada and S. Komaki, "Pre-DFT combining space diversity assisted COFDM," *IEEE Trans. Veh. Technol.*, vol. 50, pp. 487–496, Mar. 2001.

[5] D. Bartolomé and A. I. Pérez-Neira, "MMSE techniques for space diversity receivers in OFDM-based wireless LANs," *IEEE J. Select. Areas Commun.*, vol. 21, pp. 151–160, Feb. 2003.

[6] H. Matsuoka and H. Shoki, "Comparison of pre-FFT and post-FFT processing adaptive arrays for OFDM systems in the presence of co-channel interference," in *Proc. IEEE International Symposium on Personal, Indoor and Mobile Radio Communications*, vol. 2, Beijing, China, Sept. 2003, pp. 1603–1607.

[7] Z. Lei and F. P. S. Chin, "Post and pre-FFT beamforming in an OFDM system," in *Proc. IEEE 59th Vehicular Technology Conference*, vol. 1, Milan, Italy, May 2004, pp. 39–43.

[8] V. Venkataraman, R. E. Cagley, and J. J. Shynk, "Adaptive beamforming for interference rejection in an OFDM system," in *Proc. IEEE Conference Record of the Thirty-Seventh Asilomar Conference on Signals, Systems and Computers*, vol. 1, Pacific Grove, CA, Nov. 2003, pp. 507–511.

[9] J. C. Liberti and T. S. Rappaport, *Smart Antennas for Wireless Communications: IS-95 and Third Generation CDMA Applications.* Prentice Hall, 1999.

[10] J. Capon, "High-resolution frequency-wavenumber spectrum analysis," *Proc. IEEE*, vol. 57, pp. 1408–1418, Aug. 1969.

[11] T.-J. Shan and T. Kailath, "Adaptive beamforming for coherent signals and interference," *IEEE Trans. Acoustics, Speech, and Signal Processing*, vol. 33, pp. 527–536, June 1985.

[12] H. Cox, R. Zeskind, and M. Owen, "Robust adaptive beamforming," *IEEE Trans. Acoustics, Speech, and Signal Processing*, vol. 35, pp. 1365–1376, Oct. 1987.

[13] L. J. Griffiths and C. W. Jim, "An alternative approach to linearly constrained adaptive beamforming," *IEEE Trans. Antennas and Propagation*, vol. 30, pp. 27–34, Jan. 1982.

[14] A. Luthra, "A solution to the adaptive nulling problem with a look-direction constraint in the presence of coherent jammers," *IEEE Trans. Antennas and Propagation*, vol. 34, pp. 702–710, May 1986.

[15] V. Reddy, A. Paulraj, and T. Kailath, "Performance analysis of the optimum beamformer in the presence of correlated sources and its behavior under spatial smoothing," *IEEE Trans. Acoustics, Speech, and Signal Processing*, vol. 35, pp. 927–936, July 1987.

[16] K. Buckley, "Spatial/spectral filtering with linearly constrained minimum variance beamformers," *IEEE Trans. Acoustics, Speech, and Signal Processing*, vol. 35, pp. 249–266, Mar. 1987.

[17] Y.-Y. Cheng, Y. Lee, and H.-J. Li, "Subspace-MMSE blind channel estimation for multiuser OFDM with receiver diversity," in *Proc. IEEE Global Telecommunications Conference*, vol. 4, San Francisco, CA, Dec. 2003, pp. 2295–2299.

[18] C.-Y. Chi and C.-Y. Chen, "Blind beamforming and maximum ratio combining by kurtosis maximization for source separation in multipath," in *Proc. IEEE Workshop on Signal Processing Advances in Wireless Communications*, Taoyuan, Taiwan, Mar. 2001, pp. 243–246.

[19] C.-Y. Chi, C.-Y. Chen, C.-H. Chen, and C.-C. Feng, "Batch processing algorithms for blind equalization using higher-order statistics," *IEEE Signal Processing Mag.*, vol. 20, pp. 25–49, Jan. 2003.

[20] C.-Y. Chi, C.-C. Feng, C.-H. Chen, and C.-Y. Chen, *Blind Equalization and System Identificaiton.* London: Springer, 2006.

[21] C.-Y. Chi, C.-H. Chen, and C.-Y. Chen, "Blind MAI and ISI suppression for DS/CDMA systems using HOS-based inverse filter criteria," *IEEE Trans. Signal Processng*, vol. 50, pp. 1368–1381, June 2002.

[22] C.-H. Peng, C.-Y. Chi, and C.-W. Chang, "Blind multiuser detection by kurtosis maximization for asynchronous multi-rate DS/CDMA systems," *EURASIP J. Applied Signal Processing*, vol. 2006, article ID 84930, 17 pages, 2006.

[23] S. Tsumura and S. Hara, "Design and performance of quasi-synchronous multi-carrier CDMA system," in *Proc. IEEE 54th Vehicular Technology Conference*, vol. 2, Atlantic City, NJ, Oct. 2001, pp. 843–847.

[24] C.-Y. Chi and C.-H. Peng, "Turbo source extraction algorithm and noncancellation source separation algorithms by kurtosis maximization," *IEEE Trans. Signal Processing*, vol. 54, pp. 2929–2942, Aug. 2006.

[25] J. K. Tugnait, "Identification and deconvolution of multichannel linear non-Gaussian processes using higher order statistics and inverse filter criteria," *IEEE Trans. Signal Processing*, vol. 45, pp. 658–672, Mar. 1997.

[26] Z. Ding, "A new algorithm for automatic beamforming," in *Proc. IEEE Conference Record of the Twenty-Fifth Asilomar Conference on Signals, Systems and Computers*, Pacific Grove, CA, Nov. 1991, pp. 689–693.

[27] Z. Ding and T. Nguyen, "Stationary points of a kurtosis maximization algorithm for blind signal separation and antenna beamforming," *IEEE Trans. Signal Processing*, vol. 48, pp. 1587–1596, June 2000.

[28] O. Shalvi and E. Weinstein, "Super-exponential methods for blind deconvolution," *IEEE Trans. Inform. Theory*, vol. 39, pp. 504–519, Mar. 1993.

Chong-Yung Chi received the Ph.D. degree in Electrical Engineering from the University of Southern California in 1983. From 1983 to 1988, he was with the Jet Propulsion Laboratory, Pasadena, California. He has been a Professor with the Department of Electrical Engineering since 1989 and the Institute of Communications Engineering (ICE) since 1999 (also the Chairman of ICE for 2002–2005), National Tsing Hua University, Hsinchu, Taiwan. He co-authored a technical book, Blind Equalization and System Identification, published by Springer 2006, and published more than 140 technical (journal and conference) papers. His current research interests include signal processing for wireless communications, and statistical signal processing.

Dr. Chi is a senior member of IEEE. He has been a Technical Program Committee member for many IEEE sponsored workshops, symposiums and conferences on signal processing and wireless communications, including co-organizer and general co-chairman of IEEE SPAWC 2001, and Co-Chair of Signal Processing for Communications Symposium, ChinaCOM 2008. He was an Associate Editor of IEEE TRANSACTIONS ON SIGNAL PROCESSING (5/2001–4/2006), IEEE TRANSACTIONS ON CIRCUITS AND SYSTEMS II (1/2006–12/2007) and an editor (7/2003–12/2005) and a Guest Editor (2006) of EURASIP JOURNAL ON APPLIED SIGNAL PROCESSING. Currently, he is an Associate Editor for the IEEE SIGNAL PROCESSING LETTERS, an Associate Editor for the IEEE TRANSACTIONS CIRCUITS AND SYSTEMS I, and a member of Editorial Board of EURASIP SIGNAL PROCESSING JOURNAL, and a member of IEEE Signal Processing Committee on Signal Processing Theory and Methods.

Chun-Hsien Peng was born in Taiwan, on November 21, 1978. He received the B.S. degree from the Department of Electronic Engineering, National Taipei University of Technology, Taipei, Taiwan, in 2001, and the Ph.D. degree from the Institute of Communications Engineering and Department of Electrical Engineering, National Tsing Hua University, Hsinchu, Taiwan, in 2006. Since January 2007, he has been with MediaTek Incorporated, Hsinchu, where he works on the analysis, design, and implementation of the transceiver in worldwide interoperability for microwave access (WiMAX) systems. His research interests include statistical signal processing, digital signal processing, and wireless communications.

Kuan-Chang Huang was born in Kaohsiung, Taiwan, on December 19, in 1981. He received the B.S. degree from the Department of Electrical Engineering in 2004 and M.S. degree from the Institute of Communications Engineering and Department of Electrical Engineering, in 2006, National Tsing Hua University, Hsinchu, Taiwan. His research interests include digital signal processing and wireless communications.

Teng-Han Tsai was born in Taiwan, on January 1, 1982. He received the B.S. from the department of Electrical Engineering, National Tsing Hua University, Hsinchu, Taiwan, in 2005, and the M.S. degree from the Institute of Communications Engineering and Department of Electrical Engineering, National Tsing Hua University, Hsinchu, Taiwan, in 2007. His research interests include digital signal processing and wireless communications.

Wing-Kin Ma (M'01) received the B.Eng. (with first-class hons.) in electrical and electronic engineering from the University of Portsmouth, Portsmouth, U.K., in 1995, and the M.Phil. and Ph.D. degrees, both in electronic engineering, from the Chinese University of Hong Kong (CUHK), Hong Kong, in 1997 and 2001, respectively.

He is currently an Assistant Professor in the Department of Electronic Engineering, CUHK. He was with the Department of Electrical Engineering and the Institute of Communications Engineering, National Tsing Hua University, Taiwan, also as an Assistant Professor, from Aug. 2005 to Aug. 2007. He is still holding an adjunct position there. Prior to becoming a faculty, he held various research positions at McMaster University, Canada, CUHK, Hong Kong, and the University of Melbourne, Australia. His research interests are in signal processing and communications, with a recent emphasis on MIMO techniques and convex optimization. Since Oct. 2007, he has been appointed as Associate Editor of IEEE TRANSACTIONS ON SIGNAL PROCESS. Dr. Ma's Ph.D. dissertation was commended to be "of very high quality and well deserved honorary mentioning" by the Faculty of Engineering, CUHK, in 2001.